Improvement of Hydroxyapatite Formation Ability of Titanium-based Alloys by Combination of Acid Etching and Apatite Nuclei Precipitation

Takeshi Yabutsuka [1*], Yasutaka Kidokoro [1], Shigeomi Takai [1]

[1] Department of Fundamental Energy Science, Graduate School of Energy Science, Kyoto University, Yoshida-honmachi, Sakyo-ku, Kyoto 606-8501, Japan
[*]yabutsuka@energy.kyoto-u.ac.jp

Abstract: The authors aimed to improve hydroxyapatite formation ability of Ti6Al4V, Ti-15Mo-5Zr-3Al (TMZA) alloy, Ti-12Ta-9Nb-6Zr-3V-O alloy (Gummetal®) and commercially pure Ti (cpTi) mesh by combination of acid etching and apatite nuclei precipitation. Surfaces of specimens were etched with H_2SO_4 for pores formation on the specimens. Thus-etched specimens were soaked in an alkalinized simulated body fluid (SBF) which was adjusted at higher pH than that of conventional SBF and this solution was subsequently heated. By this treatment, apatite nuclei were precipitated in the pores of the specimens. By a soak in the conventional SBF to check hydroxyapatite formation ability, hydroxyapatite was covered the entire surfaces of the specimens within 1 day and high hydroxyapatite formation ability was successfully shown. Adhesion strength of the hydroxyapatite film formed in the above SBF test showed larger value as increasing surface roughness of the specimens by adjusting the above acid etching condition depending on the kinds of the Ti-based alloys. This is because the adhesion of the hydroxyapatite film was occurred by mechanical interlocking effect. In addition, this method showed shape selectivity of the materials because similar hydroxyapatite formation ability could be introduced to the cpTi mesh.

1. Introduction

It is well known that Ti metals and its oxides display unique and attractive material properties in various industrial applications. For example, Ti metals are well biocompatible because titanium oxide film is spontaneously formed on the surface of Ti metal. Thus-formed titanium oxide film not only protects Ti metals against corrosion but also improves affinity to living bone of Ti metals. In addition, titanium oxide has been commercially used especially as white pigment in paints, colorants, plastics, coatings, cosmetics, and so on [1]. Recently, furthermore, it has been also reported that some kinds of titanium oxide showed antimicrobial activity [2]. Thus, Ti-based materials possess attractive possibilities to advance wide range of clinical and industrial applications.

Ti-based alloys are the most general metallic dental or orthopaedic materials because of their excellent mechanical performance, corrosion resistance, low cost, and so on. For example, Ti6Al4V is the most typical metallic implant material because its mechanical strength is superior than that of commercially pure Ti (cpTi). However, Ti6Al4V contains vanadium with cytotoxicity and its Young's modulus is significantly higher than that of living bone. From this reason, many researchers have studied the development of novel kinds of Ti-based alloys with improved mechanical and biological properties. For example, Ti-15Mo-5Zr-3Al (TMZA) is one of the alternative candidates which does not contain cytotoxic vanadium in its metallic component and possesses higher tensile strength and lower Young's modulus than the Ti6Al4V [3] and standardized to International Standards Organization (ISO) specification 5832-14 [4]. In addition, Ti-12Ta-9Nb-6Zr-3Al-O (Gummetal®) has been also developed as super elastic and shape memory Ti-based alloy [5].

In the research field of metallic biomaterials, it is well known that Ti implanted in bone defects shows osseointegration, that is, Ti can attach with bone tissues in an optical microscopic level [6]. However, its bioactivity, that is, the biological properties that materials implanted in bone defects form hydroxyapatite (HAp) film on their surfaces spontaneously and bond to bone tissues strongly through the HAp film, is significantly lower than that of typical bioactive ceramics such as Bioglass® [7], glass ceramic A-W® [8] and sintered HAp [9]. In order to apply Ti-based alloys as highly bioactive artificial bone or bioactive dental devices, it is further required to develop effective surface modification methodologies to improve their bioactivity.

In these days, many types of surface modification processes for Ti-based alloys have been developed to improve their bioactivity and bonding strength with bone tissues. Among them, coatings techniques of biologically active ceramics are one of the main bioactive material designs. For example, sputtering [10], plasma spraying [11], sol-gel coatings [12], alkali and heat treatment [13-15], and acid and heat treatment [16] are one of the famous methodologies. However, the sputtering and plasma spraying require expensive equipment. The sol-gel process requires strict control of reaction atmosphere to suppress hydrolysis of reaction solution. Mechanical properties of Ti-based alloys are significantly changed at higher than 500 °C and deviate from the desired properties [17]. Therefore, it is desirable to keep mild temperature as possible in the surface modification processes of the Ti-based alloys.

In the previous study, the authors reported the preparation methodology of bioactive materials by incorporation of apatite nuclei (ApN) to completely bioinert or low bioactive materials [18]. When the specimens with fine pores were soaked in the conventional simulated body fluid (SBF) [19-21] with inorganic ion concentration and pH value nearly equal to that of blood plasma and its pH and temperature were raised, nucleation of calcium phosphate was promoted and calcium phosphate fine particles, which we refer as 'apatite nuclei' (ApN), were precipitated in the pores. Thus-treated specimens showed high HAp formation ability

regardless of whether the specimen was bioactive or completely bioinert. In fact, the authors successfully imparted high HAp formation ability to stainless steels (SUS) [22], CoCr-based alloy [23], and polyetheretherketone (PEEK) [24,25] by the above surface modification techniques although these specimens were completely bioinert. In the above case of PEEK, good bone-bonding ability introduced by the ApN was demonstrated in animal test [26].

Because the above surface modification technique could be applied to various kinds of bioinert materials, it could be applied to Ti-based alloys, too. In our previous study, the authors tried to obtain roughened surface on the cpTi and four kinds of Ti-based alloys by sandblasting process using alumina or silicon carbide grinding particles and subsequently treated with the above ApN treatment [27]. By this treatment, Ti-based alloys showed HAp formation ability within 1 day in the conventional SBF regardless of the metallic composition. Moreover, HAp film in the SBF showed high adhesive strength (>10 MPa) by mechanical interlocking effect. However, the sandblasting process potentially has a problem that it is quite difficult to remove contamination, that is, grinding particles remained on the surface of the specimen, even if washing process is applied using ultrasonic cleaner for a long time.

Based upon the above knowledge, it is required to apply acid etching for pores formation process instead of the sandblasting to prevent contamination on the implants during surface modification process. Ban et al. reported that H_2SO_4 etching was effective to form micropores on cpTi [28,29]. In our previous study, in addition, the authors successfully introduced HA formation ability to cpTi by the combination of fine pores formation by the H_2SO_4 etching and subsequent ApN treatment [30]. In order to expand a utility of the above process to not only cpTi but also various kinds of Ti-based alloys, in this study, the authors aimed to impart high HAp formation ability to three kinds of Ti-based alloys, which were Ti6Al4V as a representative biomedical alloy, TMZA as a vanadium-free alloy, and Gummetal® as a super elastic alloy, by applying the above surface modification process in which combined H_2SO_4 etching and subsequent ApN treatment.

2. Materials and Methods

2.1. Materials

Commercially Ti6Al4V (20 mm×10 mm×1 mm, NISHIMURA, Fukui, Japan), TMZA (15 mm×10 mm×3 mm, Kobe Steel, Kobe, Japan), Gummetal® specimens (20 mm×10 mm×1 mm, NISHIMURA) and cpTi mesh (φ0.10 mm×10 mm×10 mm, Nilaco, Tokyo, Japan) were used as specimens. The specimens except cpTi mesh was wet-polished using #400 SiC abrasive paper. All the specimens were washed in acetone, ethanol and pure water in an ultrasonic cleaner, and air-dried.

2.2. H_2SO_4 Etching

Pure water and 96% H_2SO_4 (Hayashi Pure Chemical, Osaka, Japan) were mixed and the Ti-6Al-V alloy, TMZA, Gummetal® and cpTi mesh were soaked in this H_2SO_4. Optimized mixing volume ratios of the H_2SO_4 and the pure water, reaction temperature, and reaction time for each specimen are shown in Table 1. After that, each specimen was washed with pure water in an ultrasonic cleaner.

Surfaces of the specimens were analysed by field emission scanning electron microscopy (SEM; SU6600, Hitachi High-Technologies, Tokyo, Japan). Before the SEM and EDX observation, gold was coated on the specimens by sputtering. Surface roughness and three-dimensional (3D) morphologies of the surface of the specimens were evaluated by ultra-precision point autofocus probe 3D measuring instrument (NH-3SP, Mitaka Kohki, Tokyo, Japan).

Table 1 Conditions of the H_2SO_4 etching.

Specimen	Mixing volume ratio H_2SO_4:H_2O	Temperature [°C]	Time [hours]
Ti6Al4V	2:3	90	1
TMZA	3:1	60	24
Gummetal®	4:1	60	24
cpTi mesh	1:9	90	24

2.3. ApN Treatment

The conventional SBF (Na^+; 142.0, K^+; 5.0, Mg^{2+}; 1.5, Ca^{2+}; 2.5, Cl^-; 147.8, HCO_3^-; 4.2, HPO_4^{2-}; 1.0, SO_4^{2-}; 0.5 mM) was prepared by the method certified in ISO specification 23317 [21] and its pH value was adjusted at 7.40 at 36.5 °C.

The pH of thus obtained conventional SBF was increased to 8.50 at 25.0 °C by dissolving Tris-buffer. This solution is denoted as 'alkalinized SBF', hereafter. The H_2SO_4-etched specimens were soaked in the alkalinized SBF and charged pressure at 200 MPa for 1 hour using cold isostatic pressing machine (CIP-SI, Kobe Steel, Kobe, Japan) to penetrate the alkalinized SBF in the pores of the specimens. Then, the alkalinized SBF was held at 70 °C for 1 day. By this treatment, the authors aimed to precipitate ApN in the pores of the specimens. Thus-treated specimens were washed with pure water and air-dried.

The surfaces of the specimens were analysed by thin film X-ray diffraction instrumentation (XRD; Rint 2500, Rigaku, Tokyo, Japan), SEM and energy dispersive X-ray analysis (EDX; Xflash® 5010, Bruker, Fitchburg, WI). The XRD measurements were carried out using Cu-Kα radiation at 50 kV, 300 mA of tube voltage and current.

2.4. SBF test

HAp formation ability of each specimen was evaluated by the method certified in ISO specification 23317 [21]. Each specimen was soaked in the conventional SBF for 1 day and 7 days. After the soak in SBF, the specimens were washed with pure water and air-dried. For the reference, Ti-based alloy specimens just after the H_2SO_4 treatment, that is, specimens without precipitation of ApN, were soaked in SBF for 14 days and the same washing and drying process were carried out.

The surfaces of the specimens were analysed by the XRD, SEM and EDX to check HAp formation on the surface of the specimens. In order to observe cross section of the Ti-based alloy specimens, the Ti-based alloy specimens soaked in SBF for 14 days were cut with a diamond wheel and

polished the cutting edge with #400 SiC abrasive paper. EDX mapping analyses of the cross section of the specimens were carried out to evaluate thickness of the HAp film formed on the specimens in SBF.

2.5. Tensile Test

Adhesion strength of the HAp film formed on the alkalinized SBF treated Ti-based alloys by the soak in the conventional SBF for 14 days was measured by a modified ASTM International specification C-633 [14,31-33]. A couple of stainless jigs (10 mm×10 mm) were fixed to the surface of each specimen using epoxy resin (Araldite®, NICHIBAN, Tokyo, Japan). Tensile load was applied by 1 $mm \cdot min^{-1}$ of crosshead speed using universal testing machine (AGS-H Autograph, Shimadzu, Kyoto, Japan) until fracture occurred and maximum stress was measured. After the tensile test, both jig-side and specimen-side fractured surfaces were analysed by SEM and EDX. In order to evaluate Ca/P atomic ratio of the HAp formed by the soak in SBF for 14 days, in addition, EDX quantitative analyses of the jig-side fractured surface were carried out using ZAF correction method.

3. Results

3.1. Materials Fabrication

Fig. 1 summarizes the 3D images of the surface of the Ti6Al4V, TMZA and Gummetal® specimens before and after the H_2SO_4 etching. Before the H_2SO_4 etching, flat surfaces were observed on all the kinds of alloys. After the H_2SO_4 etching, the roughened surfaces were observed on the surfaces of all the kinds of alloys. Especially, the TMZA obtained the most highly roughened surface among these conditions.

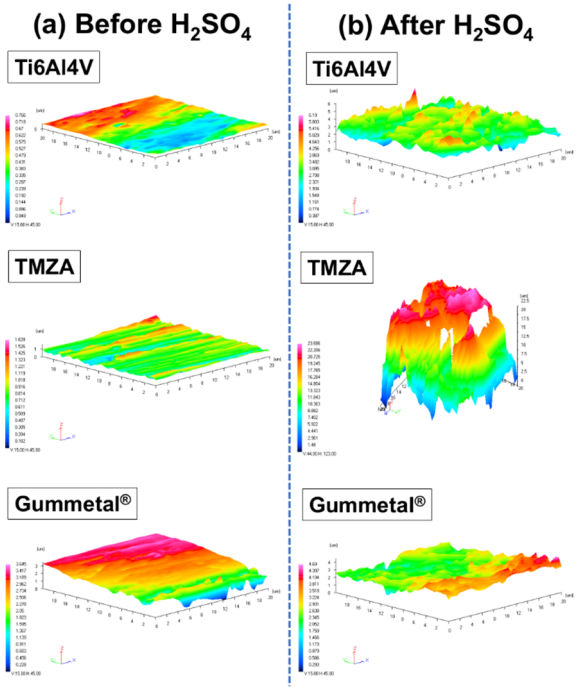

Fig. 1. *3D images of the surface of the Ti6Al4V, TMZA and Gummetal® specimens* ***(a)*** *before and* ***(b)*** *after the H_2SO_4 etching*

Table 2 summarizes the surface roughness of the Ti6Al4V, TMZA and Gummetal® specimens before and after the H_2SO_4 etching. R_a is an arithmetic average roughness. The surface roughness was increased by carrying out the above H_2SO_4 etching. The obtained surface roughness in this experimental system could be listed in order of Gummetal® < Ti6Al4V < TMZA. Especially, the TMZA obtained the significantly largest surface roughness among these alloys.

Table 2 Surface roughness (R_a) before and after the H_2SO_4 treatment.

Specimen	R_a [μm] (Before)	R_a [μm] (After)
Ti6Al4V	0.30	0.70
TMZA	0.45	11.68
Gummetal®	0.55	0.57

Fig. 2 summarizes the SEM photographs of the Ti6Al4V, TMZA and Gummetal® specimens before and after the H_2SO_4 etching. Before the H_2SO_4 etching, flat surfaces were observed on all the kinds of alloys. The observed scars were generated in the polishing process. After the H_2SO_4 etching, fine pores or the roughened surfaces were observed on the entire surfaces of the Ti6Al4V and the TMZA. However, the Gummetal® did not show such fine pores formation but slightly roughened surface.

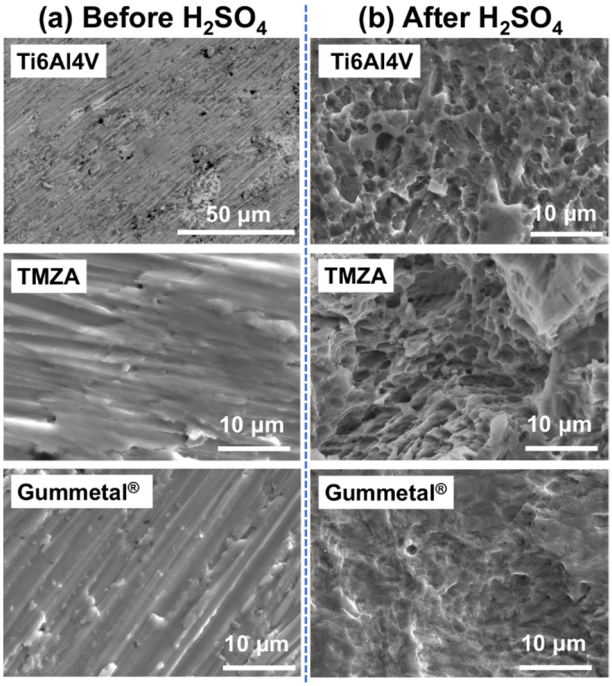

Fig. 2. *SEM photographs of the Ti6Al4V, TMZA and Gummetal® specimens* ***(a)*** *before and* ***(b)*** *after the H_2SO_4 etching*

Fig. 3 summarizes the SEM photographs and EDX spectra of the H_2SO_4-etched Ti6Al4V, TMZA and Gummetal® specimens after the soak in SBF for 14 days. Even after the soak for 14 days, morphology of the surfaces of the specimens were not changed and HAp formation was not observed. In the EDX spectra, in addition, peaks of P and Ca, constituents of HAp, were not detected. This result

indicates that HAp formation ability was not shown only by H_2SO_4 treatment of the Ti-based alloys.

Fig. 4 summarizes the SEM photographs and EDX spectra of the surfaces of the Ti6Al4V, TMZA and Gummetal® specimens after the H_2SO_4 etching and subsequent ApN treatment. Peaks of P and Ca, constituents of calcium phosphate, were observed on each sample. This result shows that ApN were precipitated near the surface of each specimen regardless of the kinds of the Ti-based alloy.

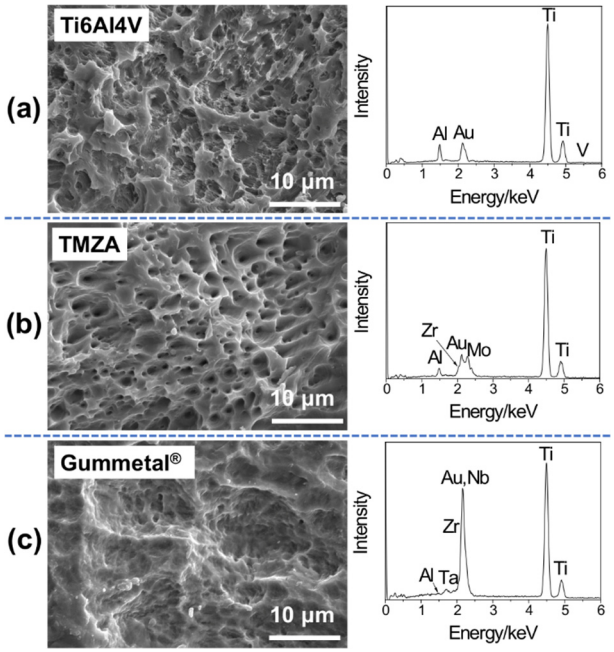

Fig. 3. *SEM photographs and EDX spectra of the H_2SO_4-etched* ***(a)*** *Ti6Al4V,* ***(b)*** *TMZA and* ***(c)*** *Gummetal® specimens after the soak in SBF for 14 days*

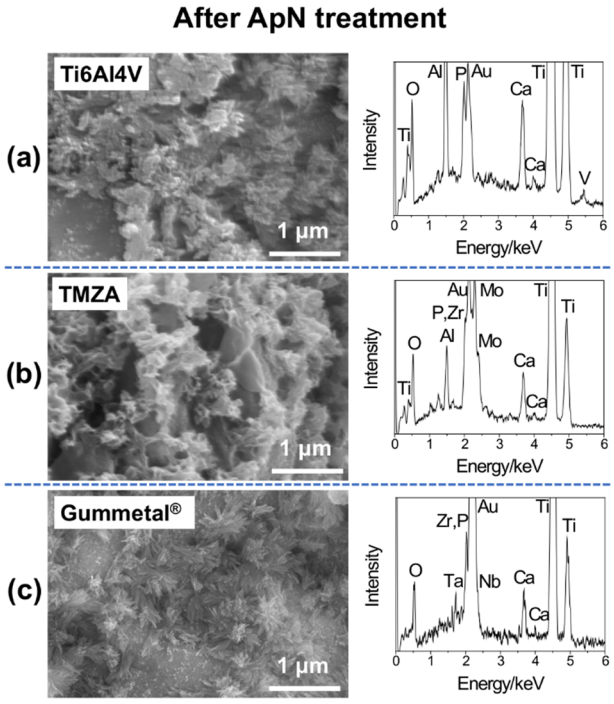

Fig. 4. *SEM photographs and EDX spectra of the surfaces of the* ***(a)*** *Ti6Al4V,* ***(b)*** *TMZA and* ***(c)*** *Gummetal® specimens after the H_2SO_4 etching and subsequent ApN treatment*

3.2. HAp Formation Ability

Fig. 5 summarizes the XRD profiles of the surfaces of the untreated, H_2SO_4, and subsequent ApN-treated Ti6Al4V, TMZA and Gummetal® specimens and those after the soak in the conventional SBF for 1 day and 7 days. Just after the ApN treatment, a broad diffraction peak of HAp was slightly observed around 32 ° for all the kinds of alloys. After the soak in the conventional SBF for 1 day, it can be seen that a number and intensity of the diffraction peaks of HAp were increased for all the types of specimens. After 7 days, they were further increased. However, it can be seen that crystallinity of the formed HAp was lower than that of general sintered HAp even after the soak in SBF for 7 days. Such low crystallinity is features of HAp formed on bioactive materials such as not only our materials but also A-W glass ceramics and NaOH and heat treated Ti metals [13-16, 19,20].

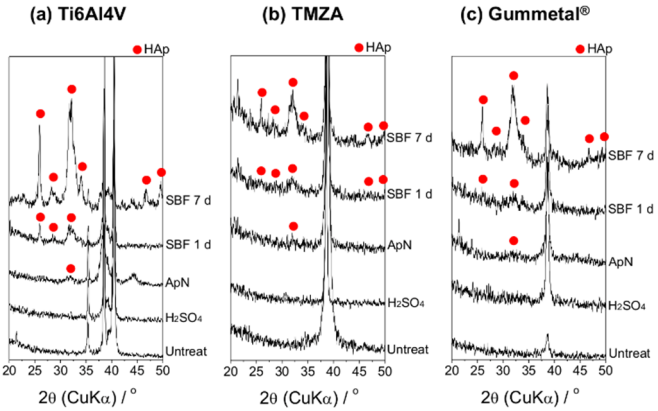

Fig. 5. *XRD profiles of the surfaces of the untreated, H_2SO_4-treated and subsequent ApN-treated* ***(a)*** *Ti6Al4V,* ***(b)*** *TMZA and* ***(c)*** *Gummetal® specimens and those after the soak in the conventional SBF for 1 day and 7 days*

Fig. 6 summarizes the SEM photographs and the EDX spectra of the surfaces of the H_2SO_4 and subsequent ApN-treated Ti6Al4V, TMZA and Gummetal® specimens after the soak in the conventional SBF for 1 day. After the soak in the conventional SBF for 1 day, it can be seen that flake-like crystallites, characteristic to HAp formed on the surfaces of bioactive materials in the conventional SBF, were covered their entire surfaces for all the kinds of alloys. This indicates that HAp formation was induced by the ApN in the conventional SBF and subsequently covered the entire surfaces of alloy specimens in the conventional SBF within 1 day and high HAp formation ability was demonstrated on the surface of each alloy.

Fig. 7 summarizes the EDX mapping images of the cross sections of the H_2SO_4 and subsequent ApN-treated Ti6Al4V, TMZA and Gummetal® specimens after the soak in the conventional SBF for 14 days. These images show that area where both Ca and P were detected were corresponded to the HAp film formed in SBF and that where Ti was strongly detected were corresponded to the alloy plate. For Ti6Al4V, it can be seen that HAp film with approximately 10 μm of

thickness was observed on the specimen. For TMZA, HAp film with approximately 20 μm of thickness was observed on the substrate. Moreover, it can be seen that the surface of the specimen was highly roughened in comparison with Ti6Al4V and Gummetal®. This result was corresponded to the largest surface roughness shown in Table 2. For Gummetal®, HAp film with 5~10 μm of thickness was observed on the specimen.

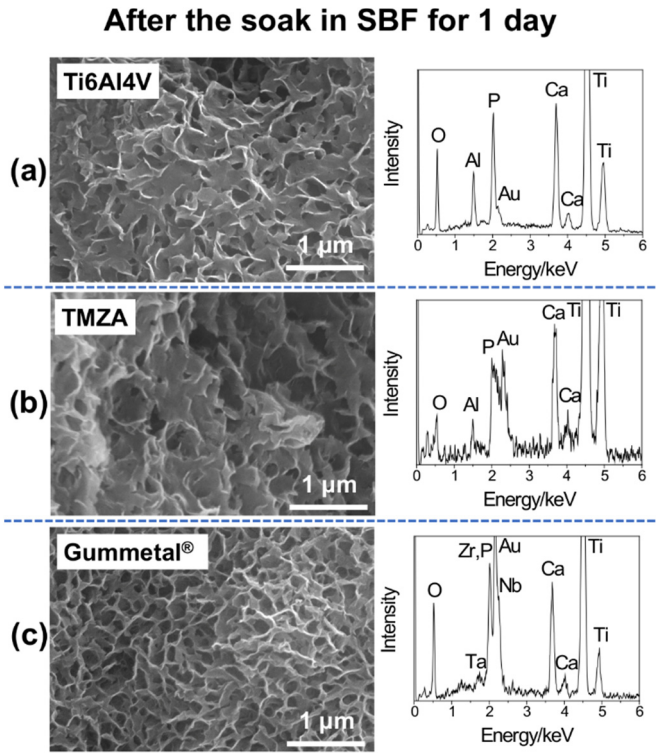

Fig. 6. *SEM photographs and EDX spectra of the surfaces of the H_2SO_4 and subsequent ApN-treated* ***(a)*** *Ti6Al4V,* ***(b)*** *TMZA and* ***(c)*** *Gummetal® specimens after the soak in the conventional SBF for 1 day*

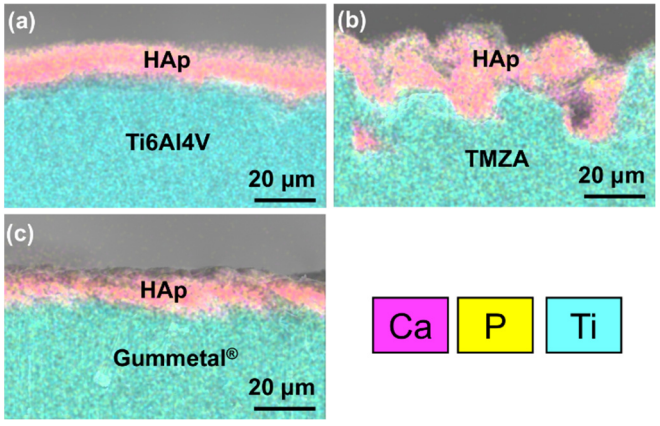

Fig. 7. *EDX mapping images of the cross sections of the H_2SO_4 and subsequent ApN-treated* ***(a)*** *Ti6Al4V,* ***(b)*** *TMZA and* ***(c)*** *Gummetal® specimens after the soak in the conventional SBF for 14 days*

3.3. Adhesion Strength of the HAp Film Formed in the SBF Test

Table 3 summarizes the average adhesion strength of the HAp film on the surface of the Ti6Al4V, TMZA and Gummetal® specimens formed by the soak in the conventional SBF for 14 days. The average adhesion strength in this experimental system could be listed in order of Gummetal®<Ti6Al4V<TMZA. Especially, the TMZA obtained the significantly largest adhesion strength (>20 MPa) among these alloys. Such tendency was corresponded to that of the surface roughness. This suggests that increase of surface roughness was the most important factor to improve the adhesion of the HAp film formed in the biological environment.

Table 3 Average adhesion strength of the HAp film formed in the SBF test (14 days soaking).

Specimen	Average (standard deviation) [MPa]
Ti6Al4V	9.2 (4.0)
TMZA	22.0 (2.9)
Gummetal®	4.4 (1.3)

Fig. 8 summarizes the SEM photographs and the EDX spectra of the jig-side fractured surfaces after the tensile test. For all the kinds of alloys, peaks of P and Ca, constituents of HAp, were strongly observed. In contrast, peaks of titanium were not observed. This indicates that HAp on the specimens were peeled off and broken of the alloy plates, on the other hand, were not occurred by the tensile test.

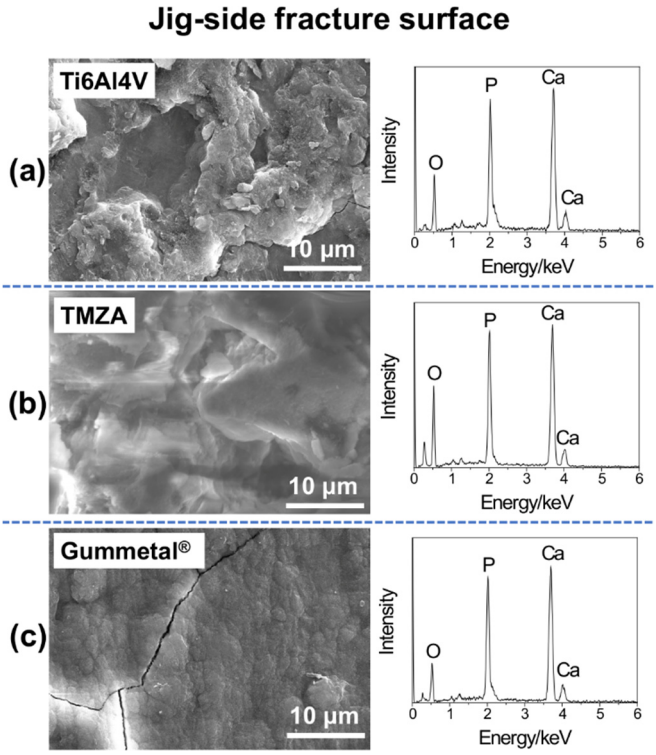

Fig. 8. *SEM photographs and EDX spectra of the jig-side fractured surfaces for* ***(a)*** *Ti6Al4V,* ***(b)*** *TMZA and* ***(c)*** *Gummetal® after the tensile test*

Fig. 9 summarizes the SEM photographs and the EDX spectra of the specimen-side fractured surfaces after the tensile test. For the Ti6Al4V and the TMZA, peaks of phosphorus and calcium, constituents of HAp, were observed. This means that fracture of HAp was occurred in the tensile test. Especially, the TMZA showed more intensified peaks of phosphorus and calcium in comparison with the Ti6Al4V. This means that a lot of fracture of the HAp was occurred on the TMZA. For the Gummetal®, in contrast, no peaks of phosphorus and calcium were detected. This means that the HAp film was almost completely peeled off and the fracture of the HAp was not occurred on the Gummetal®. Such tendency was corresponded to the result of surface roughness and adhesion strength of the HAp film.

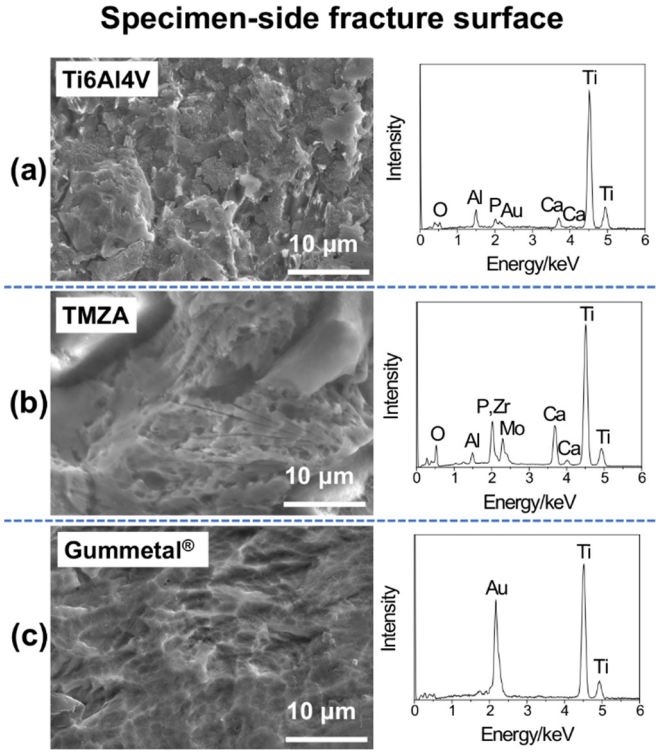

Fig. 9. *SEM photographs and EDX spectra of the specimen-side fractured surfaces for* ***(a)*** *Ti6Al4V,* ***(b)*** *TMZA and* ***(c)*** *Gummetal® after the tensile test*

Table 4 summarizes the average Ca/P atomic ratio of the HAp on the jig-side fracture surface of the Ti6Al4V, TMZA and Gummetal® specimens calculated from the results of EDX quantitative analyses. The average values were distributed around 1.62~1.68. From evaluation of significance of each value with one-way analysis of variance, significance was not found (p>0.05). It is well known that Ca/P atomic ratio of stoichiometric HAp is 1.67. It was reported that HAp formed in SBF contains minute additional inorganic ions such as Mg [20]. Hence, it is considered that the variation of the Ca/P atomic ratio in this study was derived from incorporation of these minute inorganic ions to HAp in SBF.

Table 4 Average Ca/P atomic ratio of the HAp on the jig side fracture surfaces.

Specimen	Average Ca/P atomic ratio (standard deviation)
Ti6Al4V	1.62 (0.01)
TMZA	1.68 (0.09)
Gummetal®	1.66 (0.03)
Stoichiometric HAp (Reference)	1.67

Fig. 10 (a) summarizes the SEM photographs and the EDX spectrum of the surfaces of the H_2SO_4-etched cpTi mesh. After the etching, fine pores were also observed on such fine mesh samples similar to the case of the plate samples. Fig. 10 (b) summarizes the SEM photographs and the EDX spectrum of the surfaces of the H_2SO_4 and subsequent ApN-treated cpTi mesh. In the SEM photograph in higher magnification, spherical particles were observed in the pores. In the EDX spectrum, peaks of Ca were slightly detected. This result indicates that ApN were precipitated in the pores. Fig. 10 (c) summarizes the SEM photographs and the EDX spectrum of the surfaces of the H_2SO_4 and subsequent ApN-treated cpTi mesh after soaked in the conventional SBF for 1 day. After the soak in SBF for 1 day, the cpTi mesh was covered the entire surface with flake-like crystallites of HAp. This indicate that the present method possessed shape selectivity of the specimens because the short-time HAp formation ability was shown on not only the plates but also on the fine mesh structure.

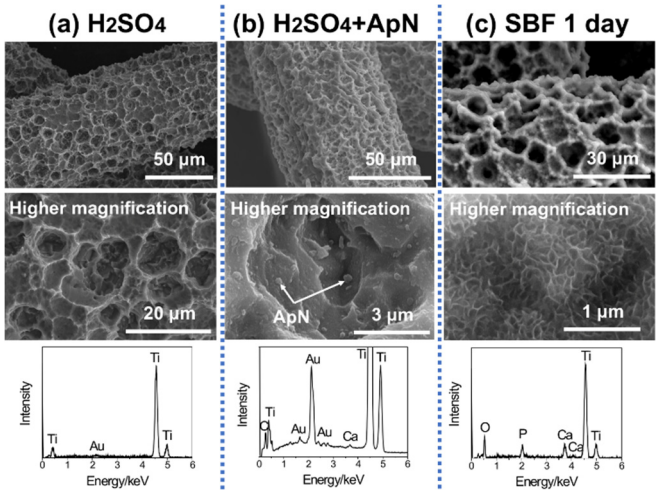

Fig. 10. *SEM photographs and EDX spectra of the surfaces of* ***(a)*** *H_2SO_4 and* ***(b)*** *subsequently ApN-treated cpTi mesh.* ***(c)*** *Those of the H_2SO_4 and subsequently ApN-treated cpTi mesh after soaked in the conventional SBF for 1 day*

4. Discussion

This report presents about novel effective treatment to introduce high HAp formation ability to various kinds of Ti-

based alloys and cpTi mesh by combination of H_2SO_4 etching and ApN treatment. The purpose of the former H_2SO_4 etching was enhancement of mechanical interlocking effect and that of the latter ApN treatment was improvement of HAp formation ability of the Ti-based alloys and cpTi mesh.

In this study, ApN precipitation condition was almost similar to bioactive PEEK and bioactive CoCr-based alloys [23-26]. This indicates that the presented bioactivity treatment possesses large materials selectivity. Just after the ApN treatment, formation of HAp film was not observed. This phenomenon was observed also in above our previous studies. Generally, HAp formation in an aqueous solution can be described as shown in below.

$$10Ca^{2+} + 6PO_4^{3-} + 2OH^- \leftrightarrow Ca_{10}(PO_4)_6(OH)_2$$

When the pH value of the aqueous solution increases, HAp formation is progressed from the viewpoint of a chemical equilibration because of an increase of OH^-. In this study, the reaction was accelerated by the high temperature environment (70.0 °C) in comparison with the physiological temperature (36.5 °C). In the case of SBF, the aqueous solution contains several kinds of additional ions such as Na^+, Mg^{2+}, K^+, Cl^- and HCO_3^- beside Ca^{2+} and PO_4^{3-} or HPO_4^{2-}. Hence, it is considered that a crystallization of the deposited calcium phosphate was inhibited by an existence of these additional ions and HAp film was not formed only by the ApN treatment.

Most different point in comparison with our previous study [27] was pores formation methodology. By H_2SO_4 etching, Ti6Al4V and TMZA showed a lot of fine pores on their surfaces. Such morphological changes were observed in the case of cpTi reported by Ban et al. [28,29] and us in our previous report [30], too. This indicate that H_2SO_4 treatment was effective to obtain fine pores not only cpTi but also Ti6Al4V and TMZA by optimizing the etching condition. However, morphological changes in the case of Gummetal® was relatively smaller than the other two kinds of alloys even if the optimization of the etching was carried out. It is speculated that this is because that the Gummetal® includes a large amount of stable metallic components such as tantalum and niobium. In this experimental step, the authors are considering that HF etching might be more effective to improve surface roughness of the Gummetal® instead of the H_2SO_4 etching because HF is easier to dissolve tantalum and niobium than H_2SO_4 [34].

Similar to our previous studies, this study also clarified that the ApN treatment was effective to introduce HAp-forming ability to the Ti-based alloys regardless of their metallic compositions because the HAp formation was induced within 1 day in the conventional SBF. It was reported that the NaOH and heat-treated Ti, which is in clinical use as hip joint, induced HAp formation within 1 day in the conventional SBF [15]. In addition, it was reported that cpTi treated with mixed acid including H_2SO_4 as main component and subsequently heated also showed HAp formation ability within 1 day in SBF [16]. Therefore, it is suggested that HAp formation ability of the Ti-based alloys treated with the ApN prepared in this study was almost comparative level. In addition, the author also presented that sandblasted Ti-based alloys showed similar level of HAp formation ability in the conventional SBF by formation of ApN [27]. From these knowledges, it is considered that HAp formation ability was affected by the ApN treatment almost exclusively and the effect of the H_2SO_4 etching was extremely small at least in the present etching condition to the HAp formation ability.

Cross-sectional observation of the Ti-based alloy specimens after the soak in SBF suggested that the thickness of the HAp film showed relationship with the surface roughness of the specimen, that is, larger surface roughness enhanced HAp formation in SBF. It is considered that this is because amount of precipitated and kept ApN in the pores became larger when the surface roughness and surface area became larger.

This study also introduces the suggestion about the relationship between the surface roughness and the adhesion strength of the HAp film formed in the conventional SBF test. From the results, it was clarified that the specimen with larger surface roughness showed larger adhesion strength of the HAp film. This tendency can be emphasized by the experimental results that TMZA which showed largest surface roughness showed significantly highest adhesion strength of the HAp film and a lot of broken HAp generated by the tensile load were remained on its specimen-side fractured surface. Hence, it is considered that the adhesion of the HAp film was largely affected by mechanical interlocking effect between the specimens and the HAp grown in the fine pores in the case of the bioactive Ti-based alloys fabricated by this method. Such consideration can be supported by also highly roughened surface morphology of TMZA clarified by cross-sectional observation. Our bioactive materials design was supported by HAp formation ability of the attached ApN in the pores of the Ti-based alloys almost exclusively instead of the oxide film formed by chemical treatment such as the NaOH-heat treatment and acid-heat treatment. Therefore, it is considered that the formed HAp film observed in this study adhered to the alloy mechanically, not chemically. Hence, the above relationship between the surface roughness and the adhesion of the HAp film is considered as one of the most important factors together with high HAp formation ability of the ApN in our bioactive materials design.

The authors acknowledge three limitations in the present study. First, condition of the H_2SO_4 treatment could not be integrated among each Ti-based alloy. Hence, simple judgement related to the kinds of the Ti-based alloys could not be done. However, the authors previously reported that the bioactivity treatment using ApN have presented in the case of not only Ti-related materials but also completely bioinert materials such as SUS [22] and CoCr-based alloy [23]. This knowledge means that the presented methodology possessed large materials selectivity. If the suitable control of the surface roughness will be possible depending on the metallic composition of the Ti-based alloys, hence, it is considered that superiority of the bioactivity and adhesion property will be almost similar. Second, the authors have not operated cell activity test to evaluate bioactivity in vitro yet. Third, the authors have not operated animal test to evaluate bone-bonding ability yet. The authors clarified, however, the bioactive PEEK fabricated by similar methodology [24,25] showed good bone-bonding ability and demonstrated effectivities of the ApN treatment to introduce bioactivity to bioinert implant materials by animal test [26]. It is well known that Ti showed osseointegration in living body, hence, the above bioactive Ti-based alloys is expected to show high

bioactivity also in living body. These points will be studied in our next opportunity.

5. Conclusion

The surfaces of Ti6Al4V, TMZA, Gummetal®, and cpTi mesh were etched by H_2SO_4. The specimens were soaked in the alkalinized SBF and raised its temperature. By this treatment, ApN were precipitated in the pores of the specimen. Thus-treated specimens showed HAp formation ability in a short period. Adhesion strength of the HAp film formed in the conventional SBF became larger as increasing the surface roughness of the specimen by optimizing the above H_2SO_4 etching condition. This is because the adhesion of the hydroxyapatite film was improved by enhancement of mechanical interlocking effect in this materials design.

6. Acknowledgments

This work was partly supported by Iketani Science and Technology Foundation (ISTF), LNest Grant from Leave a Nest Co., Ltd., and Kyoto University Supporting Program for Interaction-based Initiative Team Studies (SPIRITS).

7. References

[1] Zeman, T., Loh, E.W., Cierny, D., et al.: 'Penetration, Distribution and Brain Toxicity of Titanium Nanoparticles in Rodents' Body: A Review', IET Nanobiotechnol., 2018, 12, (6), pp 695-700

[2] Abdul Jalill R.D.: 'Green Synthesis of Titanium Dioxide Nanoparticles with Volatile Oil of Eugenia caryophyllata for Enhanced Antimicrobial Activities', IET Nanobiotechnol., 2018, 12, (5), pp 678-687

[3] Okazaki, Y.: 'Selection of metals for biomedical devices', in Niinomi, M. (Ed.): 'Metals for Biomedical Devices' (Woodhead Publishing, 2019, 2nd edn.), pp 31-94

[4] ISO 5832-14: 'Implants for Surgery—Metallic Materials—Part 14: Wrought titanium 15-molybdenum 5-zirconium 3-aluminium alloy', 2019

[5] Saito, T., Furuta, T., Hwang, J.H., et al.: 'Multifunctional Alloys Obtained via a Dislocation-Free Plastic Deformation Mechanism', Science, 2003, 300, (5618), pp 464-467

[6] Larsson, C., Esposito, M., Liao, H., et al.: 'The Titanium-Bone Interface In Vivo'., in Brunette, D.M., Tengvall, P., Textor, M., et al. (Ed.): 'Titanium in Medicine' (Springer, 2001), pp 587-648

[7] Hench, L.L.: 'Bioceramics: From Concept to Clinic', J. Am. Ceram. Soc., 1991, 74, (7), pp 1487-1510

[8] Kokubo, T., Shigematsu, M., Y. Nagashima, Y., et al.: 'Apatite- and Wollastonite-Containg Glass-Ceramics for Prosthetic Application', Bull. Inst. Chem. Res. Kyoto Univ., 1982, 60, (3-4), pp 260-268

[9] Jarcho, M., Kay, J.F., Gumaer, K.I., et al.: 'Tissue, cellular and subcellular events at a bone-ceramic hydroxylapatite interface', J. Bioeng., 1977, 1, (2), pp 79-82

[10] Cooley, D.R., van Dellen, A.F., Burgess, J.O., et al.: 'The advantages of coated titanium implants prepared by radiofrequency sputtering from hydroxyapatite', J. Prosthet. Dent., 1992, 67, (1), pp 93-100

[11] de Groot, K., Geesink, R., Klein, C.P.A.T., et al.: 'Plasma sprayed coatings of hydroxylapatite', J. Biomed. Mater. Res., 1987, 21, (12), pp 1375-1387

[12] Peltola, T., Pätsi, M., Rahiala, H., et al.: 'Calcium phosphate induction by sol-gel-derived titania coatings on titanium substrates in vitro', J. Biomed. Mater. Res., 1998, 41, (3), pp 504-510

[13] Kim, H.-M., Miyaji, F., Kokubo, T., et al.: 'Preparation of bioactive Ti and its alloys via simple chemical surface treatment', J. Biomed. Mater. Res., 1996, 32, (3), pp 409-417

[14] Kim, H.-M., Miyaji, F., Kokubo, T., et al.: 'Bonding strength of bonelike apatite film to Ti metal substrate', J. Biomed. Mater. Res., 1997, 38, (2), pp 121-127

[15] Kim, H.-M., Miyaji, F., Kokubo, T., et al.: 'Bonding strength of bonelike apatite film to Ti metal substrate', J. Biomed. Mater. Res., 1997, 38, (2), pp 121-127

[16] Kokubo, T., Pattanayak, D.K., Yamaguchi, S., et al.: 'Positively charged bioactive Ti metal prepared by simple chemical and heat treatments', J. R. Soc. Interface, 2010, 7, pp S503-S513

[17] Ikeda, M., Komatsu, S., Sugimoto, T., et al.: 'Effect of two phase warm rolling on aging behavior and mechanical properties of TMZA', Mater. Sci. Eng. A, 1998, 243, (1), pp 140-145

[18] Yao, T., Hibino, M., Yabutsuka, T.: 'Method of producing bioactive complex material', U.S. Patent, 2013, 8512732, Japanese Patent, 2013, 5252399

[19] Kokubo, T., Kushitani, H., Sakka, S., et al.: 'Solutions able to reproduce in vivo surface-structure changes in bioactive glass-ceramic A-W', J. Biomed. Mater. Res., 1990, 24, (6), pp 721-734

[20] Kokubo, T., Takadama, H.: 'How useful is SBF in predicting in vivo bone bioactivity?', Biomaterials, 2006, 27, (15), pp. 2907-2915

[21] ISO 23317: 'Implants for Surgery—In vitro evaluation for apatite-forming ability of implant materials', 2014

[22] Yabutsuka, T., Karashima, R., Takai, S., et al.: 'Effect of Doubled Sandblasting Process and Basic Simulated Body Fluid Treatment on Fabrication of Bioactive Stainless Steels', Materials, 2018, 11, (8), 1334

[23] Yabutsuka, T., Mizutani, H., Takai, S., et al.: ‘Fabrication of Bioactive Co-Cr-Mo-W Alloy by Using Doubled Sandblasting Process and Apatite Nuclei Treatment’, Trans. Mat. Res. Soc. Japan, 2018, 43, (3), pp 143-147

[24] Yabutsuka, T., Fukushima, K., Hiruta, T., et al.: ‘Effect of pores formation process and oxygen plasma treatment to hydroxyapatite formation on bioactive PEEK prepared by incorporation of precursor of apatite’, Mater. Sci. Eng. C: Mater. Biol. Appl., 2017, 81, pp 349-358

[25] Yabutsuka, T., Fukushima, K., Hiruta, T., et al.: ‘Fabrication of Bioactive Fiber-reinforced PEEK and MXD6 by Incorporation of Precursor of Apatite’, J. Biomed. Mater. Res. B: Appl. Biomater., 2018, 106, (6), pp 2254-2265

[26] Masamoto, K., Fujibayashi, S., Yabutsuka, T., et al.: ‘In vivo and in vitro bioactivity of a "precursor of apatite" treatment on polyetheretherketone’, Acta Biomater., 2019, 91, pp 48-59

[27] Yabutsuka, T., Mizuno, H., Takai, S.: ‘Fabrication of bioactive titanium and its alloys by combination of doubled sandblasting process and alkaline simulated body fluid treatment’, J. Ceram. Soc. Japan, 2019, 127, (10), pp 669-677

[28] Ban, S., Taniki, T., Sato, H., et al.: ‘Acid Etching of Titanium for Bonding with Veneering Composite Resins’, Dent. Mater. J., 2006, 25, (2), pp 382-390

[29] Ban, S., Iwaya, Y., Kono, H., et al.: ‘Surface modification of titanium by etching in concentrated sulfuric acid’, Dent. Mater., 2006, 22, (12), pp 1115-1122

[30] Yabutsuka, T., Hibino, M., Yao, T., et al.: ‘Fabrication of Bioactive Apatite Nuclei Precipitated Titanium by Using Electromagnetic Induction Heating’, Bioceram. Dev. Appl., 2011, 1, D110122

[31] Lacefield, W.R.: ‘Hydroxyapatite Coatings’, in Hench, L.L. (Ed.): ‘An Introduction to Bioceramics’ (Imperial College Press, 2013, 2nd edn.), pp 331-347

[32] Miyazaki, T., Kim, H.-M., Kokubo, T., et al.: ‘Enhancement of bonding strength by graded structure at interface between apatite film and bioactive tantalum metal’, J. Mater. Sci. Mater. Med., 2002, 13, (7), pp 651-655

[33] Juhasz, J.A., Best, S.M., Kawashita, M., et al.: ‘Bonding strength of the apatite film formed on glass-ceramic apatite-wollastonite-polyethylene composites’, J. Biomed. Mater. Res. A, 2003, 67, (3), pp 952-959

[34] Schweitzer, P.A.: ‘Corrosion Engineering Handbook’ (CRC Press, 2006, 2nd edn.)